RSC Advances

ROYAL SOCIETY OF CHEMISTRY

www.rsc.org/advances

The effect of co-doping nano-SiO_2 and nano-Al_2O_3 on the improved performance of poly(methyl methacrylate-acrylonitrile-ethyl acrylate) based gel polymer electrolyte for lithium ion battery

Ping Sun [a], Youhao Liao [a,b*], Xueyi Luo [a], Zihao Li [a], Tingting Chen [a], Lidan Xing [a], Weishan Li [a,b*]

[a] *School of Chemistry and Environment, South China Normal University, Guangzhou 510631, China*

[b] *Engineering Research Center of MTEES (Ministry of Education), Research Center of BMET (Guangdong Province), and Key Laboratory of ETESPG (GHEI), South China Normal University, Guangzhou 510631, China.*

Abstract

In this article, we report a novel gel polymer electrolyte (GPE) for lithium ion battery, which is prepared by using poly(methyl methacrylate-acrylonitrile-ethyl acrylate) (P(MMA-AN-EA)) as polymer matrix and doping nano-SiO_2 and nano-Al_2O_3 simultaneously. The influences of the ratio of two nanoparticles on the pore structure, electrolyte uptake and thermal stability of the resulting membrane and the ionic conductivity and electrochemical stability of the corresponding GPE are understood by scanning electron microscopy, mechanical strength, thermogravimetry, electrochemical impedance spectroscopy, linear sweep voltammetry and cyclic voltammetry. Particularly, the performance of the developed GPE for its application in lithium ion battery is evaluated in Li/$LiNi_{0.5}Mn_{1.5}O_4$ half cell by charge/discharge test. It is found that there exists a synergistic effect between nano-SiO_2 and

∗ School of Chemistry and Environment, South China Normal University, Guangzhou 510006, China. Tel/fax: 86-20-39310256.
E-mail address: liaoyouhao@126.com (Y.H. Liao), liwsh@scnu.edu.cn (W.S. Li)

nano-Al_2O_3. The performances of the resulting membrane and the corresponding GPE are effectively improved by using nano-SiO_2 and nano-Al_2O_3 simultaneously than individually. Co-doping 5 wt.% nano-SiO_2 and 5 wt.% nano-Al_2O_3 provides the membrane with a higher thermally decomposed temperature of 325 ^oC and a better electrolyte uptake of 198.1%, the corresponding GPE with an increased ionic conductivity of 2.2×10^{-3} $S.cm^{-1}$ at room temperature and an enhanced oxidative stability up to 5.5 V (*vs.* Li/Li^+), and the $LiNi_{0.5}Mn_{1.5}O_4$ cathode with an improved rate capability of 104.2 $mAh.g^{-1}$ at 2 C and an improved capacity retention of 94.8% after 100 cycles. These improved performances result from the combining advantages of both nano-SiO_2 and nano-Al_2O_3, in which the former contributes to the improved ionic conductivity caused by stronger Lewis-acid property, while the latte to the better thermal and structural stability by its stiffness characterization.

Keywords: Synergistic effect; Nanoparticles co-doped; Poly(methyl methacrylate-acrylonitrile-ethyl acrylate); Gel polymer electrolyte; Lithium ion battery.

1. Introduction

Secondary lithium ion battery has been widely used in portable device for energy storage due to its high energy density and friendly environmental effect since its commercialization in 1990s [1-9], and the demand for lithium ion battery is increasing quickly as the rapid development of electric vehicles and hybrid-electric vehicles (EVs and HEVs) [10,11]. However, it remains a challenge to avoid the potential danger in the applications of lithium ion battery, which is caused by the oxidation decomposition of liquid organic electrolytes, especially when high voltage cathodes are used [12-14].

Among the diverse electrolytes, gel polymer electrolyte (GPE) is thought to be one of the effective ways to solve the safety problem and to extend the narrow oxidative potential of liquid organic electrolyte. In GPE, the free movement of liquid electrolyte is restricted

through swelling the organic electrolyte into the suitable polymer matrixes, leading to the improved stability of electrolyte [15-18]. However, there are some problems need to be solved before GPE can be applied in large scale to commercial battery, such as lowly ionic conductivity and unsatisfactory rate performance [19-21].

Developing new polymer matrix is proved to be effective to enhance the comprehensive performance of the corresponding GPE. Based on our previous research, the characterization of GPE using terpolymers [poly(methyl methacrylate-acrylonitrile-ethyl acrylate), poly(methyl methacrylate-acrylonitrile-vinyl acetate), poly(acrylonitrile-methyl methacrylate-styrene)] is much promoted compared with that of bi-polymers in the form of poly(methyl methacrylate-acrylonitrile), poly(methyl-methacrylate-vinyl acetate), poly(acrylonitrile-vinyl acetate) and poly(butyl meth-acrylate-styrene) [22-28].

Doping proper amount of inorganic nanoparticles in the polymer matrix is another effective strategy to improve the performance of GPEs [29-32]. Inorganic nanoparticles, on one hand, provide transportation paths for lithium ion due to their Lewis-acid property, contributing to the increased ionic conductivity. On the other hand, they provide GPEs with enhanced mechanical strength and dimensional stability because of the better thermal and structural stability of inorganic oxides than polymers. Among the inorganic nanoparticles that have been reported in GPEs, nano-Al_2O_3 and nano-SiO_2 are believed to be most effective for the performance improvement of GPEs [33,34]. Our groups have chosen these two kinds of nanoparticles as additives in the GPE system. The satisfied results, such as better electrochemical stability, higher ionic conductivity, good compatibility with lithium anode and excellent cycle stability, are exhibited in previous reports. Interesting, it has been found that the GPEs with 10 wt.% nanoparticles exhibit the best performances. The involved GPEs include nano-SiO_2 doped poly(butyl methacrylate-styrene) GPE [26], poly (methyl methacrylate-acrylonitrile-vinyl acetate) (P(MMA–AN–VAc)) [35] and poly(methyl

methacrylate-co-butyl acrylate) [36] based GPEs, and nano-Al_2O_3 doped poly(methyl methacrylate-vinyl acetate)-*co*-poly(ethylene glycol) diacrylate [37], poly(ethylene oxide)-poly(vinylidene fluoride-hexafluoropropylene) [38] and poly(acrylonitrile-co-methyl methacrylate) [39] based GPEs. Recently, we have compared the contributions of nano-SiO_2 and nano-Al_2O_3 to the performance improvement in P(MMA–AN–VAc) based GPE and found that SiO_2 based GPE has better compatibility with anode than Al_2O_3 based GPE, which can be attributed to the stronger Lewis-acid property of SiO_2, while the stiffness characterization of Al_2O_3 leads to the better thermal stability [40].

However, there is less researches on the influence of the co-doping inorganic nanoparticles in the GPE system. Synergistic effect has been reported for the co-doped metallic oxide into the cathode, such as the electrochemical characterization improvement of $LiNi_{0.5}Mn_{1.5}O_4$ cathode by co-doping Co and Cr [41]. Here, synergistic effect implicates that the performance of co-doping Co and Cr sample is significantly enhanced compared that of the samples individually doping Co or Cr. Thus, we expect that the performance of GPE will be improved more effectively by doping nano-SiO_2 and nano-Al_2O_3 simultaneously than individually, and synergistic effect may happen if the performance of co-doped sample is better than that of the individual one. Accordingly we developed a novel GPE by using poly(methyl methacrylate-acrylonitrile-ethyl acrylate) (P(MMA-AN-EA)) as polymer matrix and doping nano-SiO_2 and nano-Al_2O_3 simultaneously. The influences of the ratios of two nanoparticles on the pore structure, electrolyte uptake and thermal stability of the resulting membrane and the ionic conductivity of the corresponding GPE were understood in this paper. Particularly, the performance of the developed GPE for its application in lithium ion battery was evaluated with $LiNi_{0.5}Mn_{1.5}O_4$, a representative high-voltage cathode.

2. Experimental

2.1 Preparation

Polymer poly(methyl methacrylate-acrylonitrile-ethyl acrylate) (P(MMA-AN-EA)) with monomer mass ratio of MMA:AN:EA = 4:2:1 was synthesized by emulsion polymerization. This ratio was chosen based on the formation convenience and the performance reliability of membrane in our previous report [22]. The total content of nanoparticles in the polymer was kept to be 10 wt.%. The synthesized polymer P(MMA–AN–EA) and 10 wt.% nanoparticles were dissolved in dimethylformamide (DMF) at 80 ^{o}C for 1 hour to form a slurry containing 3 wt.% polymer and nanoparticles. The mass ratios of nano-SiO_2 (Aladdin, 99.5%, average particle size 30 nm) and nano-Al_2O_3 (Aladdin, 99.9%, α-Al_2O_3 with average particle size of 30 nm) was 10:0, 7.5:2.5, 5:5, 2.5:7.5, and 0:10, the resulting samples were marked as MS10, MS7.5, MS5, MS2.5 and MS0, respectively. For comparison, the sample without nanoparticle was also obtained and labeled as M0.

The resulting viscous slurry was cast with a doctor blade onto both sides of polyethylene (PE) separator, and then transferred into deionized water for 2 hours to induce phase inversion. The resulting membrane was washed with running water, dried in vacuum at 60 ^{o}C for 24 hours and the porous membrane with average thickness of 80 μm was obtained finally. In order to prepare GPE, the membrane was immersed in a liquid electrolyte, 1 M $LiPF_6$ in ethylene carbonate (EC) / dimethyl carbonate (DMC) (1/1, v/v, battery grade, Samsung Cheil Industry, Korea) for 0.5 hour in an argon-filled glove box (MBRAUN).

Cathode electrode was fabricated by mixing the active material of $LiNi_{0.5}Mn_{1.5}O_4$, conductive agent of carbon black and binder of polyvinylidene fluoride (PVDF) in the weight ratios of 80:10:10. N-methylpyrrolidone (NMP) was applied as a solvent to prepare the electrode slurry. CR2025 type coin cell in the structure of Li/GPE/$LiNi_{0.5}Mn_{1.5}O_4$ was assembled in argon-filled glove box to evaluate the cathode performance when nanoparticles

co-doped GPE was used.

2.2 Characterization

The morphology of the developed membranes was examined with scanning electron microscope (SEM, JEOL, JSM-6510, Japan). The mechanical property of the membranes was determined by microcomputer control electron universal testing machine (model CMT6104). The thermal stability of the membranes was measured with thermogravimetric analyzer (TGA, Perkin-Elmer TGA7) under N_2 atmosphere from room temperature to 600 ^oC at a heating rate of 10 $^oC.min^{-1}$. The membranes (diameter Φ = 18 mm) were immersed into the liquid electrolyte for half an hour and then the excess electrolyte on the surface was removed by pressing lightly between two sheets of filter paper with a weight of 50 g on the top of the upper filter paper. The electrolyte uptake (A) of the membranes was calculated according to Eq. 1,

$$A(\%) = \frac{W_2 - W_1}{W_1} \times 100\% \quad (1)$$

where W_1 and W_2 were the mass of the dry and wet membrane, respectively.

The GPE was sandwiched between two parallel stainless steel (SS) discs (diameter Φ = 16.2 mm) in order to characterize the ionic conductivity by electrochemical impedance spectroscopy (EIS) on electrochemical instrument (Metrohm Autolab PGSTAT302N, the Netherlands) using alternative current signal with potential amplitude of 10 mV and frequencies from 100 kHz to 1 Hz. The ionic conductivity was calculated from the bulk electrolyte resistance (R) based on Eq. 2,

$$\sigma = \frac{l}{RS} \quad (2)$$

where l was the thickness of the GPE, S the contact area between GPE and SS disc.

The activation energy (E_a) of the GPE for the lithium ion transfer was obtained from Eq. 3,

$$\sigma = A\exp(-\frac{E_a}{kT}) \quad (3)$$

where σ was the ionic conductivity, T the absolute temperature, A the pre-exponential constant and k the Boltzmann constant.

EIS was carried out to characterize the interfacial stability between the GPE and Li metal electrode. Li/GPE/Li type of symmetrical structure was fabricated by sandwiching the GPE between two lithium electrodes and measured through alternative current signal with potential amplitude of 5 mV and frequencies from 500 kHz to 0.03 Hz. The electrochemically oxidative stability of the GPE was determined in the cell type of Li/GPE/SS by linear sweep voltammetry (LSV) using the scanning rate of 1 $mV.s^{-1}$ on Metrohm Autolab (PGSTAT302N, the Netherlands). The Li electrode was used as the reference and the counter electrodes, while the SS as working electrode. Cyclic voltammetry (CV) was used to determine the reversible deposition and dissolution of lithium ion on the developed GPE. The measurement was carried out on an electrochemical workstation (Solartron Analylical 1470E, England) and scanned at rate of 1 $mV.s^{-1}$ with the coin cell structure of SS/GPE/Li in the voltage range of -0.5 V ~ 5 V. The SS was applied as working electrode and the lithium as the reference and the counter electrodes.

The coin cells comprising of Li/GPE/$LiNi_{0.5}Mn_{1.5}O_4$ were tested on charge/discharge instrument (Land CT2001A, Wuhan Land Electronic Co. Ltd, China) between 3.5 V and 5.0 V at room temperature. The coin cells were cycled at 0.1 C within 3 cycles in the same cyclic voltage range to activate the cathode before cyclic stability test, while at 0.05 C for 5 cycles for rate ability evaluation. The theory capacity of $LiNi_{0.5}Mn_{1.5}O_4$ cathode extracted one Li in unit cell is 146.7 $mAh.g^{-1}$.

3. Results and discussion

3.1 Morphology of membranes

Fig. 1 shows the SEM images of PE-supported P(MMA-AN-EA) membranes without and with different mass ratios of nano-SiO_2 and nano-Al_2O_3. The M0 membrane without nanoparticle has poor structure that pores are dispersed non-uniformly on the surface. Nanoparticles seem to induce the formation of porous membranes, and more pores can be observed on the surface of the membrane and the interconnected structure is also present for all of the samples after doping different species. Based on our previous studies [35,38-40], the membrane doped with 10 wt.% of nanoparticle exhibited comprehensive performance, higher level led to agglomerate, resulted from the naturally branched structure of nano-size particles [42]. The MS10 membrane, the one with nano-SiO_2, has a large number of pores on the uneven surface and the interconnected structure can be observed under the surface. After introducing 2.5 wt.% nano-Al_2O_3 as the secondary phase into the membrane, the MS7.5 sample keeps the interconnected and porous structure with the uniform pore size, which should be ascribed to the different property of electric charges for nano-SiO_2 and nano-Al_2O_3. Due to the repulsive interaction between nano-SiO_2 and nano-Al_2O_3, the nanoparticles disperse uniformly in the MS7.5 membrane. Decreasing the content of nano-SiO_2 to the amount of nano-Al_2O_3, the MS5 membrane shows the best uniform structure in the form of proper pore size with average diameter of about 0.5 μm. For MS2.5 membrane, with 2.5 wt.% nano-SiO_2, the pore number descends and the pore structure tends to become compact with reduced pore diameter, which is unbeneficial for holding the liquid electrolyte effectively. Among the doped membranes, the most compact pore structure and the least pore number is MS0 membrane, with 10 wt.% nano-Al_2O_3 individually. Comparing MS10 with MS0, it can be found that the porous structure of the membrane is also affected by the species of nanoparticles. Doping nano-SiO_2 in the polymer matrix seems to present bigger diameter of porous size, which is in according with our previous studies that doping nano-SiO_2 into P(MMA–AN–VAc) based membrane exhibits better performance than that of nano-Al_2O_3. On the other hand, there is a synergistic

effect of co-doping nanoparticles in the improvement of the porous structure in the co-doped membrane, especially for the MS5 membrane, which presents best porous structure.

3.2 Thermal stability

Thermal stability of membrane is one of the key factors that determine the safety of lithium ion battery. Fig. 2 presents TG curves of P(MMA-AN-EA) based membranes with different contents of nanoparticles. Here, the decomposition temperature is defined at the temperature that losses its original weight larger than 3 wt.%. It can be seen from Fig. 2 that the membranes doped with nanoparticles have higher decomposition temperature than the membrane without nanoparticles, although the shape of TG curves is similar. P(MMA-AN-EA) based membrane is thermally stable up to 300 ^{o}C, while much higher decomposed temperature of 325 ^{o}C can be observed for all the membranes doped by the different contents of nano-SiO_2 and nano-Al_2O_3. Furthermore, the short plateaus among 375-400 ^{o}C are observed for four kinds of membranes, caused by the thermal decomposition of supporter-polyethylene membrane [43, 44]. These observations indicate that doping nanoparticles does improve the thermal stability of the membrane. The bond in the polymer membrane is strengthened by adding the nanoparticle that contains the active -Si-O bond or -Al-O bond, which reacts with the polymer chains to form complex bonds. During the heating procedure, the polymer membrane is decomposed by breaking down the inside bond of polymer chain, such as -C-H, -C≡N. The improved bond strength that modified by the -Si-O or -Al-O group in the chains enhances the thermally decomposed temperature of membrane subsequently. On the other hand, the melting point of nanoparticle is much higher than that of the polymer, which is also contributed to the improvement in the thermal stability of membrane consecutively. Especially, the membrane containing nano-Al_2O_3 individually has the best thermal toleration, suggesting that the nano-Al_2O_3 contributes to the thermal stability

by its original stiffness characterization.

3.3 Mechanical strength

Mechanical property is an important factor to determine the fabricated characterization of the commercial lithium ion battery, which is measured by the elongation strength of membrane. Fig. 3 shows the mechanical strength of the MS0, MS5 and MS10 membranes. The fracture strength of MS5 membrane (46.9 MPa) is higher than that of the MS0 and the MS10. Thus, the developed membranes are sufficient application in the practical usage of lithium ion battery.

3.4 Electrolyte uptake

Fig. 4 shows the wettability of PE-supported P(MMA-AN-EA) membranes with different mass ratios of nano-SiO_2 and nano-Al_2O_3 in the same process time of 15 seconds after applying a drop of liquid electrolyte in an argon-filled glove box. For the PE membrane as support, a dew bead can be observed clearly. However, the liquid electrolyte is quickly spread out although there are not much difference among the prepared membranes, suggesting that the wettability of polymer membranes is significantly improved by coating polymer and nanoparticle onto the PE support. This improved wettability results from the better affinity of polymer to the polar carbonated electrolyte because of the C=O and C≡N groups in the polymer chains. Similar finding has been reported for the other copolymer membrane [43,44].

Fig. 5 presents the dependence of the electrolyte uptake ability on the different membranes. It can be seen from Fig. 5 that the electrolyte uptake of membrane is closely related to its pore structure. The electrolyte uptake of M0 membrane has the lowest value (102.2%). The uptake ability for all the membranes is enhanced by doping proper amount of nanoparticles. As also presented in Fig. 5, the electrolyte uptake of membrane doped with nano-SiO_2 is higher than

that of the membrane doped with nano-Al_2O_3 individually, indicating that nano-SiO_2 contributes more positively to the electrolyte uptake caused by its stronger Lewis-acid property. Furthermore, the uptake ability for co-doping membranes is also further enhanced. Exhilaratingly, the MS5 membrane has the highest electrolyte uptake (198.1%), ascribed to its best interconnected structure that the pores is uniform and owns proper size, which is beneficial to retain the liquid electrolyte effectively.

3.5 Ionic conductivity

Fig. 6 presents the Nyquist plots of the P(MMA–AN–EA)-based GPEs with different mass ratios of nanoparticles at room temperature. According to Eq. 2, the calculated ionic conductivity for the developed GPEs is also presented in Fig. 6. It can be found that the ionic conductivity is almost proportional to the electrolyte uptake that is originally affected by the pore structure of membrane. The ionic conductivity of GPEs with different nanoparticles is always higher than that of the M0 GPE. The huge surface area of nanoparticles helps to form the better pore structure that stores liquid electrolyte effectively, providing more routes for the ionic transportation. Besides, the nanoparticles play a positive role for the migration of lithium ion by forming the cross-linked centers, and the tendency of polymer chain reorganization for the doped GPE is also lower compared with the non-doped one, leading to the enhancement of the ionic conductivity by improving the structural stiffness after structure modification [39]. Moreover, the ionic conductivity for GPE doped by nano-SiO_2 individually has larger value than that doped by nano-Al_2O_3 alone. According to the Lewis acid-base theory, the Lewis acid strength of nano-SiO_2 is stronger than nano-Al_2O_3. The competition of the Lewis acid between nanoparticle and Li-ion forces $LiFP_6$ salt to dissociate more Li-ion, while the stronger Lewis acid of nano-SiO_2 promotes the dissociated rate, leading to the enhancement of ionic conductivity. The largest ionic conductivity of 2.2×10^{-3} $S\cdot cm^{-1}$ belongs

to the MS5 GPE, which is higher than that of the M0 GPE, whose value is 1.2×10^{-3} S·cm^{-1} at room temperature. It should pay attention to that the ionic conductivity of the MS5 is still higher than the MS10 or MS0, caused by the synergistic effect of co-doping nanoparticles, which is related to the properly porous structure and the higher uptake of liquid electrolyte.

From the discussion above, the optimal MS5 GPE is used to further investigate the synergistic effect of co-doping nano-SiO_2 and nano-Al_2O_3. As comparison, the MS10, MS0 and M0 are also selected.

In order to clearly understand the conductive mechanism of the GPEs, the ionic conductivity is investigated under different temperatures. From Fig. 7, it can be verified that the ionic conductivity of GPEs with different nanoparticles has the same tendency on the reciprocal temperature, which increases linearly with the absolute temperature. This conductive behavior obviously follows Arrhenius law. Adding nanoparticles into the polymer do not change the conductive mechanism of the GPE. Based on Eq. 3, the value of the active energy (E_a) can be calculated by the slope of the fitting lines in the temperature range of 348 K to 298 K. As shown in Table 1 the doped GPEs have much lower E_a than the M0 GPE, indicating that the rate of Li-ion transportation is speeded up after doping. The E_a of MS10 GPE is lower than that of the MS0 GPE, which should be ascribed to the stronger interaction between nano-SiO_2 and polymer matrix that facilitates the diffusion and migration of lithium ion. As also presented in Table 1, the lowest E_a is observed for the MS5 GPE, whose value is 9.6 kJ.mol^{-1}. Lower E_a means lower barrier for the diffusion and migration of lithium ion, resulting from the temporary transition point produced by the nanoparticle, and the co-dopants increase the effective connected point.

3.6 Electrochemical stability

Irreversibly oxidative decomposition of liquid electrolyte takes place over the potential

than 4.4 V (*vs.* Li/Li^+) using the commercial $LiCoO_2$ as cathode when the outside circuit of battery suffers from the overcharge condition, which is deleterious to the battery and even causes safety hazards. Thus, it is especially important to understand the oxidative stability of developed electrolyte to avoid overcharging the battery. Fig. 8 presents the decomposed potential for the different electrolytes. The obtained result for the PE membrane saturated with the liquid electrolyte indicates that the oxidative decomposition happens at the potential of about 4.4 V (*vs.* Li/Li^+), which is ascribed from the lowly oxidative stability of the solvent components in organic liquid electrolyte. Much higher oxidative potential can be observed for the GPEs. The M0 GPE is electrochemically stable up to about 4.9 V. After adding nanoparticles, the oxidative stability is significantly improved for all the GPEs although different species are doped, whose current onset in the anodic region begins at 5.5 V. Notably, the decomposed potential of MS5 GPE is as high as 5.6 V.

The interaction between P(MMA-AN-EA) polymer and liquid electrolyte restricts the free movement of liquid component by gelatinization process. Adding nanoparticle individually to the GPE, the Si-O bond or Al-O bond as the connected point, contributes to build stronger polymer network structure by the formation of Si-O-C or Al-O-C covalent bonds, the interaction between polymer and liquid electrolyte is strengthened sequentially. The complementary function of the Si-O bond and Al-O bond makes the interaction between polymer and liquid electrolyte become tight enough, which is built through connecting the center of Si-O bond and Al-O bond for the super network structure, while inconsistently electronic charge between SiO_2 and Al_2O_3 promotes the quality and the effectively connected points between polymer and liquid electrolyte. Thus, the best oxidative stability of MS5 GPE is presented by the synergistic effect of co-doping.

Fig. 9 shows the cyclic voltammogram (CV) of various GPEs for the cell Li/GPEs/SS scanned at the voltage range of -0.5 V ~ 5 V. Four samples has the similar trend, in which has

no obvious current response between 1.0 V and 5.0 V, while presents strong redox peaks concerning about the decomposition and precipitation of lithium ions in the voltage range of -0.5 V ~1.0 V. The peaks in the first five cycles are almost overlapped, indicating the reversible process for the deposition and dissolution of lithium ions. The CV measurement is also in accordance with the results of linear sweep voltammograms that the developed GPEs are electrochemically stable up to 5 V, which are good candidate for the potential application in the 5 V high voltage cathodes.

3.7 Compatibility with lithium anode

The compatibility of GPE with lithium anode was estimated by the interfacial behavior of a coin cell Li/GPE/Li. Fig. 10 (a) shows the dependence of interfacial resistance of diverse GPEs on the storage time at open circuit. Take MS5 GPE as example to illustrate the electrochemical impedance spectroscopy (EIS), as shown in Fig. 10 (b), the Nyquist plots are presented in a depressed semicircular arc in the high frequency range and a short line in the low frequency scope, while the diameter of depressed semicircle is considered as the interfacial resistance between the GPE and lithium electrode. It can be found from Fig. 10 (a) that the interfacial resistance of the M0 GPE increases quickly after the 15 days, however, much lower increased magnitude can be observed for the GPEs doped by nanoparticles. The MS10 GPE shows lower increased magnitude than MS0 GPE. The surface of nanoparticle contains hydroxyl groups, which can further react with a small quantity of H_2O in the liquid electrolyte through forming the hydrogen bonds, and then the encapsulated trace H_2O becomes lazy to react with the lithium metal, leading to stabilize the interface between the GPE and lithium metal. Nano-SiO_2 has stronger complexing ability for absorbing small amount of H_2O to inhibit the major side reactions, contributing to the smaller interfacial resistance.

MS5 GPE has the lowest increased magnitude, whose resistance value increases from 51.9 $\Omega.cm^2$ on the first day to 63.1 $\Omega.cm^2$ after the 15 days, indicating that the interfacial stability of GPE can be further improved by co-doped nanoparticles. Because of the incongruously electric charges property, the different function of nanoparticles will compete to react with the impurities in liquid electrolyte, the unpleasantly side reaction is inhibited effectively by those nanoparticles with large specific surface area, which in turn reduce the resistance subsequently.

3.8 Cathode performance

Fig. 11 presents the rate capability of $LiNi_{0.5}Mn_{1.5}O_4$ cathode with various electrolytes at different C-rates at room temperature. The cathode is charged at the current of 0.1 C and discharged at 0.1 C, 0.2 C, 0.5 C, 1 C, 2 C for each 10 cycles, and then backs to 0.1 C to estimate the recovered ability of rate capacity. As indicated in Fig. 11, the capacity of cathode is decreased with increasing the discharged rate regardless of the electrolytes. The cathode exhibits better rate performance using the doped GPE, while the difference is magnified at the higher rate. For the MS5 GPE, the discharge capacity delivers 136.4 $mAh.g^{-1}$ at 0.1 C rate in the 10^{th} cycle, and the capacity is 135.4 $mAh.g^{-1}$ at 0.2 C in the 20^{th} cycle, while the value is reduced to 130.2 $mAh.g^{-1}$ at 0.5 C in the 30^{th} cycle. The capacity is further dropped to 104.2 $mAh.g^{-1}$ at 2 C rate in the 50^{th} cycle, which has 76.4% capacity retention of 0.1 C. Finally its capacity is fully returned to 133.1 $mAh.g^{-1}$ in the following 51^{th} cycle at the small current of 0.1 C, suggesting that the cathode can be reversibly cycled under 0.1 C. Similar trend is also observed for the other GPEs and the less capacity at different rates is assigned to M0 GPE. It can be also noted that the capacity of MS10 at 2 C is even a little higher than the MS5 GPE, due to its bigger diameter of pores that is convenient for the fast transfer of Li-ion.

Fig. 12 presents the cyclic stability of the $LiNi_{0.5}Mn_{1.5}O_4$ cathode using various electrolytes

in the voltage range of 3.5 V ~ 5.0 V under 0.2 C rate at room temperature. Although the initial capacity of the $LiNi_{0.5}Mn_{1.5}O_4$ cathode is similar for three kinds of electrolytes, the fading rate is different after cycling. The steadily declined trend is observed for the cathode using the developed GPEs. After 100 cycles, the capacity retention is 94.8% for the MS5, and 89.2% for the M0. The gelation of liquid electrolyte suppresses the decomposition of organic electrolyte at the potential over 4.4 V, and doped nanoparticles strengthen this gelation effect. However, the cyclability of $LiNi_{0.5}Mn_{1.5}O_4$ cell is not only related to the electrolyte, but also determined by the cathode itself. The reason for capacity fading of $LiNi_{0.5}Mn_{1.5}O_4$ cell is that small amount of extracted Li-ion cannot insert reversibly into the $Li_{1-x}Ni_{0.5}Mn_{1.5}O_4$ cathode during cycling.

The uniform and interconnected pore structure is beneficial to the cycliability, especially at the higher rate, which originally results from the inducing effect of doped nanoparticles. After co-doping, the GPE shows appropriate ionic conductivity, and the compatibility with lithium anode and higher anti-oxidative ability, which in turn plays a positive role on the cathode performance, so that current can disperse uniformly and the partial polarization is largely avoided, the irreversible reaction of electrolyte or cathode is restricted finally. Thus, the synergistic effect of co-doping nano-SiO_2 and nano-Al_2O_3 is obvious and strongly affects the performance of the membrane and the corresponding GPE. The results presented in this study indicate that MS5 membrane can be a promising candidate as separator for safer Li-ion battery, and the MS5 GPE is good alternative to be used in high-voltage lithium ion battery.

4. Conclusions

The synergistic effect of co-doping nano-SiO_2 and nano-Al_2O_3 on the performance of P(MMA-AN-EA) based membrane and corresponding GPE is presented in this paper. The best performance is observed for the MS5 membrane and corresponding GPE that contains 5

wt.% nano-SiO_2 and 5 wt.% nano-Al_2O_3 because of the synergistic effect. Here, nano-SiO_2 contributes to the improved ionic conductivity caused by stronger Lewis-acid property, while nano-Al_2O_3 to the better thermal and structural stability by its stiffness characterization. The MS5 membrane exhibits the interconnected structure with suitable pore size, which is beneficial to uptake the liquid electrolyte effectively, leading to the enhancement of the ionic conductivity. Subsequently, the synergistic effect of co-doping nano-SiO_2 and nano-Al_2O_3 should give a bright stimulation to develop better performance of inorganic ceramic membrane doped together with different functional nanoparticles.

Acknowledgements

The authors are grateful for the financial support from the joint project of the National Natural Science Foundation of China and Natural Science Foundation of Guangdong Province (Grant No. U1401248), the National Natural Science Foundation (Grant No. 21403076), Natural Science Foundation of Guangdong Province (Grant No. 2014A030310324), the key project of Science and Technology in Guangdong Province (Grant Nos. 2012A090300012 and 2013B090800013), and the scientific research project of Department of Education of Guangdong Province (Grant No. 2013CXZDA013).

References

[1] L. Wang, H.-J. Zhu, W. Zhai, F. Cai, X.-M. Liu and H. Yang, Study of a novel gel electrolyte based on poly-(methoxy/hexadecyl-poly(ethylene glycol) methacrylate) co-polymer plasticized with 1-butyl-3-methylimidazolium tetrafluoroborate, *RSC Adv.*, 2014, 4, 36357-36365.

[2] Y. Zhu, S. Xiao, Y. Shi, Y. Yang, Y. Hou and Y. Wu, A composite gel polymer electrolyte with high performance based on poly(vinylidene fluoride) and polyborate for lithium ion

batteries, *Adv. Energy Mater.*, 2014, 4, 1-9.

[3] T. F. Yi, Y. Xie, L. J. Jiang, J. Shu, C.-B. Yue, A.-N. Zhou and M.-F. Ye, Advanced electrochemical properties of Mo-doped $Li_4Ti_5O_{12}$ anode material for power lithium ion battery, *RSC Adv.*, 2012, 2, 3541–3547.

[4] J.L. Shi, L.F. Fang, H. Li, H. Zhang, B.K. Zhu and L. P. Zhu, Improved thermal and electrochemical performances of PMMA modified PE separator skeleton prepared via dopamine-initiated ATRP for lithium ion batteries. *J. Membrane Sci.*, 2013, 437, 160-168.

[5] S. Dalavi, M. Xu, L. Zhou, B. Ravdel, and B.L. Lucht, Nonflammable electrolytes for lithium-ion batteries containing dimethyl methylphosphonate, *J. Electrochem. Soc.*, 2010, 157: A1113-A1120.

[6] P. Zhu, Y. Wu, M. V. Reddy, A. Sreekumaran Nair, B. V. R. Chowdari and S. Ramakrishna, Long term cycling studies of electrospun TiO_2 nanostructures and their composites with MWCNTs for rechargeable Li-ion batteries, *RSC Adv.*, 2012, 2, 531–537.

[7] R. Miao, J. Yang, X. Feng, H. Jia, J. Wang and Y. Nuli, Novel dual-salts electrolyte solution for dendrite-free lithium-metal based rechargeable batteries with high cycle reversibility, *J. Power Sources*, 2014, 271, 291-297.

[8] Q. Lu, J. Fang, J. Yang, G. Yan, S. Liu and J. Wang, A novel solid composite polymer electrolyte based on poly(ethylene oxide) segmented polysulfone copolymers for rechargeable lithium batteries, *J. Membrane Sci.*, 2013, 425-426, 105-112.

[9] Y. Wang, L. Xing, X. Tang, X. Li, W. Li, B. Li, W Huang, H. Zhou and X. Li, Oxidative stability and reaction mechanism of lithium bis(oxalate)borate as a cathode film-forming additive for lithium ion batteries, *RSC Adv.*, 2014, 4, 33301-33306.

[10] H.B. Lin, H.B. Rong, W.Z. Huang, Y.H. Liao, L.D. Xing, M.Q. Xu, X.P. Li and W.S. Li, Triple-shelled Mn_2O_3 hollow nanocubes: force-induced synthesis and excellent performance as the anode in lithium-ion batteries, *J. Mater. Chem. A*, 2014, 2:

14189-14194.

[11] H.B. Lin, Y.M. Zhang, H.B. Rong, S.W. Mai, J.N. Hu, Y.H. Liao, L.D. Xing, M.Q. Xu, X.P. Li and W.S. Li, Crystallographic facet- and size-controllable synthesis of spinel $LiNi_{0.5}Mn_{1.5}O_4$ with excellent cyclic stability as cathode of high voltage lithium ion battery, *J. Mater. Chem. A*, 2014, 2: 11987-11995.

[12] D.Y. Zhou, G.Z. Wang, W.S. Li, G.L. Li, C.L. Tan, M.M. Rao and Y.H. Liao, Preparation and performances of porous polyacrylonitrile–methyl methacrylate membrane for lithium-ion batteries, *J. Power Sources*, 2008, 184: 477-480.

[13] Z.H. Li, P. Zhang, H.P. Zhang, Y.P. Wu and X.D. Zhou, A lotus root-like porous nanocomposite polymer electrolyte, *Electrochem. Commun.*, 2008, 10, 791-794.

[14] V. Etacheri, R. Marom, R. Elazari, G. Salitra and D. Aurbach, Challenges in the development of advanced Li-ion batteries: a review, *Energ. Environ. Sci.*, 2011, 4, 3243-3262.

[15] N.T. Kalyana Sundaram, O.T. Muhammed Musthafa, K.S. Lokesh and A. Subramania, Effect of porosity on PVdF-*co*-HFP–PMMA-based electrolyte, *Mater. Chem. Phys.*, 2008, 110: 11-16.

[16] G. Vijayakumar, S.N. Karthick, A.R. Sathiya Priya, S. Ramalingam and A. Subramania, Effect of nanoscale CeO_2 on PVDF-HFP-based nanocomposite porous polymer electrolytes for Li-ion batteries, *J. Solid State Electr.*, 2008, 12, 1135-1141.

[17] Z.H. Li, H.P. Zhang, P. Zhang, G.C. Li, Y.P. Wu and X.D. Zhou, Effects of the porous structure on conductivity of nanocomposite polymer electrolyte for lithium ion batteries, *J. Membrane Sci*., 2008, 322: 416-422.

[18] P. Raghavan, X. Zhao, J.K. Kim, J. Manuel, G. S. Chauhan, J. H. Ahn and C. Nah, Ionic conductivity and electrochemical properties of nanocomposite polymer electrolytes based on electrospun poly(vinylidene fluoride-co-hexafluoropropylene) with nano-sized ceramic

fillers, *Electrochim. Acta*, 2008, 54, 228-234.

[19] A. Manuel Stephan and K.S. Nahm, Review on composite polymer electrolytes for lithium batteries, *Polymer*, 2006, 47, 5952-5964.

[20] A. Manuel Stephan, Review on gel polymer electrolytes for lithium batteries, *Eur. Polym. J.*, 2006, 42, 21-42.

[21] J.Y. Song, Y.Y. Wang and C.C. Wan, Review of gel-type polymer electrolytes for lithium-ion batteries, *J. Power Sources*, 1999, 77, 183-197.

[22] P. Sun, Y. Liao, H. Xie, T. Chen, M. Rao and W. Li, Poly(methyl methacrylate-acrylonitrile- ethyl acrylate) terpolymer based gel electrolyte for $LiNi_{0.5}Mn_{1.5}O_4$ cathode of high voltage lithium ion battery, *J. Power Sources*, 2014, 269, 299-307.

[23] M.M. Rao, J.S. Liu, W.S. Li, Y. Liang and D.Y. Zhou, Preparation and performance analysis of PE supported P(AN-*co*-MMA) gel polymer electrolyte for lithium ion battery applications, *J. Membrane Sci.*, 2008, 322, 314-319.

[24] L. Lu, X.X. Zuo, M.Q. Xu, J.S. Liu and W.S. Li, Study on the preparation and performances of PMMA-Vac polymer electrolyte for lithium ion battery use, *Acta Chim. Sinica*, 2007, 65, 475-480.

[25] X.P. Li, M.M. Rao, Y.H. Liao, W.S. Li and M.Q. Xu, Non-woven fabric supported poly(acrylonitrile-vinyl acetate) gel electrolyte for lithium ion battery use, *J. Appl. Electrochem.*, 2010, 40, 2185-2191.

[26] Y.H. Liao, M.M. Rao, W.S. Li, L.T. Yang, B.K. Zhu, R. Xu and C.H. Fu, Fumed silica-doped poly(butyl methacrylate-styrene)-based gel polymer electrolyte for lithium ion battery, *J. Membrane Sci.*, 2010, 352, 95-99.

[27] Y.H. Liao, D.Y. Zhou, M.M Rao, W.S. Li, Z.P. Cai, Y. Liang and C.L. Tan, Self-supported poly (methyl methacrylate-acrylonitrile-vinyl acetate) based gel electrolyte for lithium ion

battery, *J. Power Sources*, 2009, 189, 139-144.

[28] L. Chen, M.M. Rao, W.S. Li, M.Q. Xu, Y.H. Liao, C.L. Tan and J. Yi, Performance improvement of polyethylene-supported poly (acrylonitrile-methyl methacrylate-styrene) electrolyte by using urea as foaming agent, *Acta Phys.-Chim. Sin.*, 2011, 27, 1689-1694.

[29] P.P. Prosini, P. Villano and M. Carewska, A novel intrinsically porous separator for self-standing lithium-ion batteries, *Electrochim. Acta*, 2002, 48, 227-233.

[30] H.S. Kim, K.S. Kum, W. Cho, B.W. Cho and H.W. Rhee, Electrochemical and physical properties of composite polymer electrolyte of poly(methyl methacrylate) and poly(ethylene glycol diacrylate), *J. Power Sources*, 2003, 124: 221-224.

[31] J.H. Park, W. Park, J.H. Kim, D. Ryoo, H.S. Kim, Y.U. Jeong, D.W. Kim and S.Y. Lee, Close-packed poly(methyl methacrylate) nanoparticle arrays-coated polyethylene separators for high-power lithium-ion polymer batteries, *J. Power Sources*, 2011, 196, 7035-7038.

[32] P. Zhang, H.P. Zhang, G.C. Li, Z.H. Li and Y.P. Wu, A novel process to prepare porous membranes comprising SnO_2 nanoparticles and P(MMA-AN) as polymer electrolyte, *Electrochem. Commun.*, 2008, 10, 1052-1055.

[33] Z. Li, G. Su, D. Gao, X. Wang and X. Li, Effect of Al_2O_3 nanoparticles on the electrochemical characteristics of P(VDF-HFP)-based polymer electrolyte, *Electrochim. Acta*, 2004, 49, 4633-4639.

[34] W. Li, Y. Xing, X. Xing, Y. Li, G. Yang and L. Xu, PVDF-based composite microporous gel polymer electrolytes containing a novel single ionic conductor SiO_2 (Li^+), *Electrochim. Acta*, 2013, 112, 183-190.

[35] Y. Liao, M. Rao, W. Li, C. Tan, J. Yi and L. Chen, Improvement in ionic conductivity of self-supported P(MMA-AN-VAc) gel electrolyte by fumed silica for lithium ion batteries, Electrochim. Acta, 2009, 54, 6396-6402.

[36] H. Xie, Y. Liao, P. Sun, T. Chen, M. Rao and W. Li, Investigation on polyethylene-supported and nano-SiO_2 doped poly(methyl methacrylate-co-butyl acrylate) based gel polymer electrolyte for high voltage lithium ion battery, *Electrochim. Acta*, 2014, 127, 327-333.

[37] Y.H. Liao, X.P. Li, C.H. Fu, R. Xu, M.M. Rao, L. Zhou, S.J. Hu and W.S. Li, Performance improvement of polyethylene-supported poly(methyl methacrylate-vinyl acetate)-co-poly(ethylene glycol) diacrylate based gel polymer electrolyte by doping nano-Al_2O_3, *J. Power Sources*, 2011, 196, 6723-6728.

[38] Y.H. Liao, X.P. Li, C.H. Fu, R. Xu, L. Zhou, C.L. Tan, S.J. Hu and W.S. Li, Polypropylene-supported and nano-Al_2O_3 doped poly(ethylene oxide)–poly(vinylidene fluoride-hexafluoropropylene)-based gel electrolyte for lithium ion batteries, *J. Power Sources*, 2011, 196, 2115-2121.

[39] M.M. Rao, J.S. Liu, W.S. Li, Y.H. Liao, Y. Liang and L.Z. Zhao, Polyethylene-supported poly(acrylonitrile-*co*-methylmethacrylate)/nano-Al_2O_3 microporous composite polymer electrolyte for lithium ion battery, *J. Solid State Electr.*, 2010, 191, 255-261.

[40] Y. Liao, C. Sun, S. Hu and W. Li, Anti-thermal shrinkage nanoparticles/polymer and ionic liquid based gel polymer electrolyte for lithium ion battery, *Electrochim. Acta*, 2013, 89, 461-468.

[41] D. R. Chen, B. Z. Li, Y. H. Liao, H. W. Lan, H. B. Lin, L. D. Xing, Y. T. Wang and W. S. Li, Improved electrochemical performance of $LiNi_{0.5}Mn_{1.5}O_4$ as cathode of lithium ion battery by Co and Cr co-doping, *J. Solid State Electrochem.*, 2014, 7, 2027-2033.

[42] M. Yanilmaz, Y. Lu, M. Dirican, K. Fu and X. Zhang, Nanoparticle-on-nanofiber hybrid membrane separators for lithium-ion batteries via combining electrospraying and electrospinning techniques, *J. Membrane Sci.*, 2014, 456, 57-65.

[43] J.A. Conesa, A. Marcilla, R. Font, J.A. Caballero, Thermogravimetric studies on the

thermal decomposition of polyethylene, *J. Analytical and Applied Pyrolysis*, 1996, 36, 1-15.

[44] Q. Lu, J. Fang, J. Yang, R. Miao, J. Wang and Y. Nuli, Novel cross-linked copolymer gel electrolyte supported by hydrophilic polytetrafluoroethylene for rechargeable lithium batteries, *J. Membrane Sci.*, 2014, 449, 176-183.

Figure Captions:

Fig. 1 SEM images of PE-supported P(MMA-AN-EA) membranes with different contents of nanoparitcles. M0: without nanoparticle, MS10: 10 wt.% nano-SiO_2, MS7.5: 7.5 wt.% nano-SiO_2 and 2.5 wt.% Al_2O_3, MS5: 5 wt.% nano-SiO_2 and 5 wt.% Al_2O_3, MS2.5: 2.5 wt.% nano-SiO_2 and 7.5 wt.% Al_2O_3, and MS0: 10 wt.% Al_2O_3.

Fig. 2 TG curves of P(MMA-AN-EA) membranes with different contents of nanoparticles.

Fig. 3 Mechanical strength of the MS0, MS5 and MS10 membranes.

Fig. 4 Wettability of the PE separator and PE-supported P(MMA-AN-EA) membranes with different contents of nanoparticles.

Fig. 5 Dependence of electrolyte uptake and ionic conductivity on the different types of membranes.

Fig. 6 Nyquist plots for the different GPEs in SS/GPE/SS cell at room temperature.

Fig. 7 Temperature dependence on the ionic conductivity of GPEs.

Fig. 8 Linear sweep voltammograms of various GPEs on stainless steel with the scanning rate of 1 $mV.s^{-1}$.

Fig. 9 Cyclic voltammograms of various GPEs for the cell Li/GPEs/SS in the voltage range of -0.5~5 V, scanning rate: 1 $mV.s^{-1}$.

Fig. 10 (a) The dependence of interfacial resistance of Li/GPEs on the storage time, and (b) the detail electrochemical impedance spectra for MS5 GPE.

Fig. 11 Rate capability of $LiNi_{0.5}Mn_{1.5}O_4$ in various electrolytes at room temperature.

Fig. 12 Cyclic stability of $LiNi_{0.5}Mn_{1.5}O_4$ in various electrolytes under 0.2 C rate in the voltage range of 3.5 V and 5.0 V at room temperature.

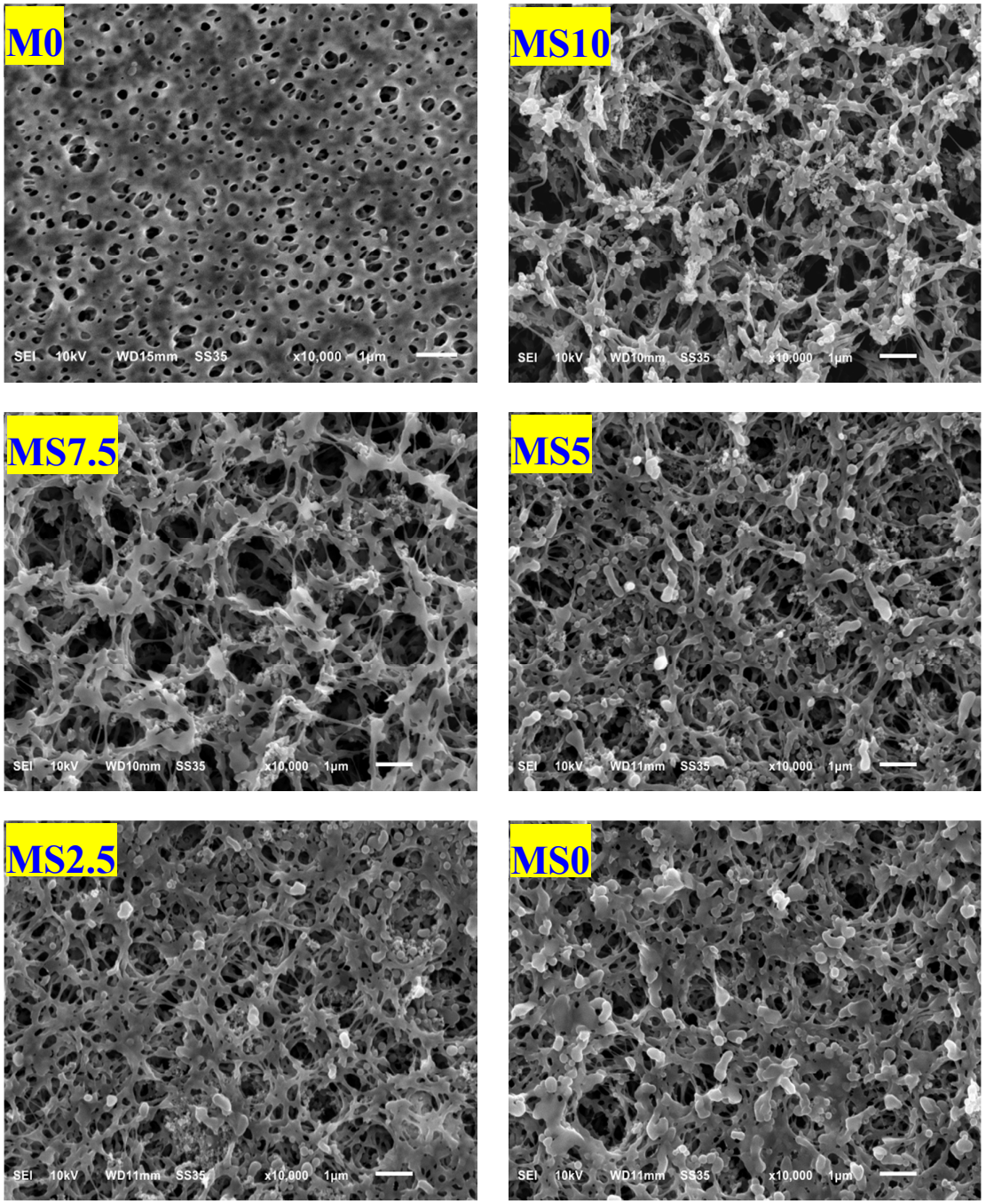

Fig. 1 SEM images of PE-supported P(MMA-AN-EA) membranes with different contents of nanoparitcles. M0: without nanoparticle, MS10: 10 wt.% nano-SiO_2, MS7.5: 7.5 wt.% nano-SiO_2 and 2.5 wt.% Al_2O_3, MS5: 5 wt.% nano-SiO_2 and 5 wt.% Al_2O_3, MS2.5: 2.5 wt.% nano-SiO_2 and 7.5 wt.% Al_2O_3, and MS0: 10 wt.% Al_2O_3.

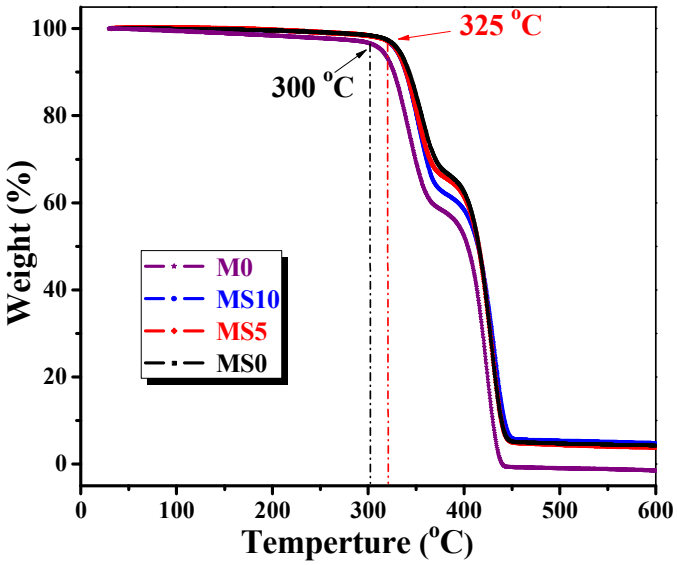

Fig. 2 TG curves of P(MMA-AN-EA) membranes with different contents of nanoparticles.

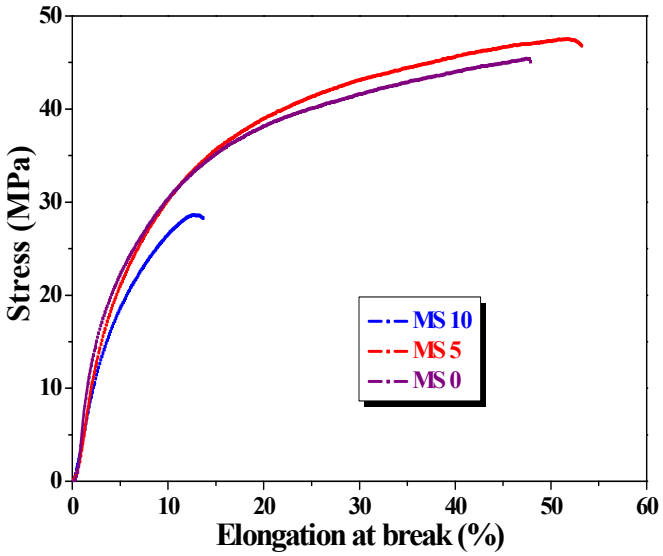

Fig. 3 Mechanical strength of the MS0, MS5 and MS10 membranes.

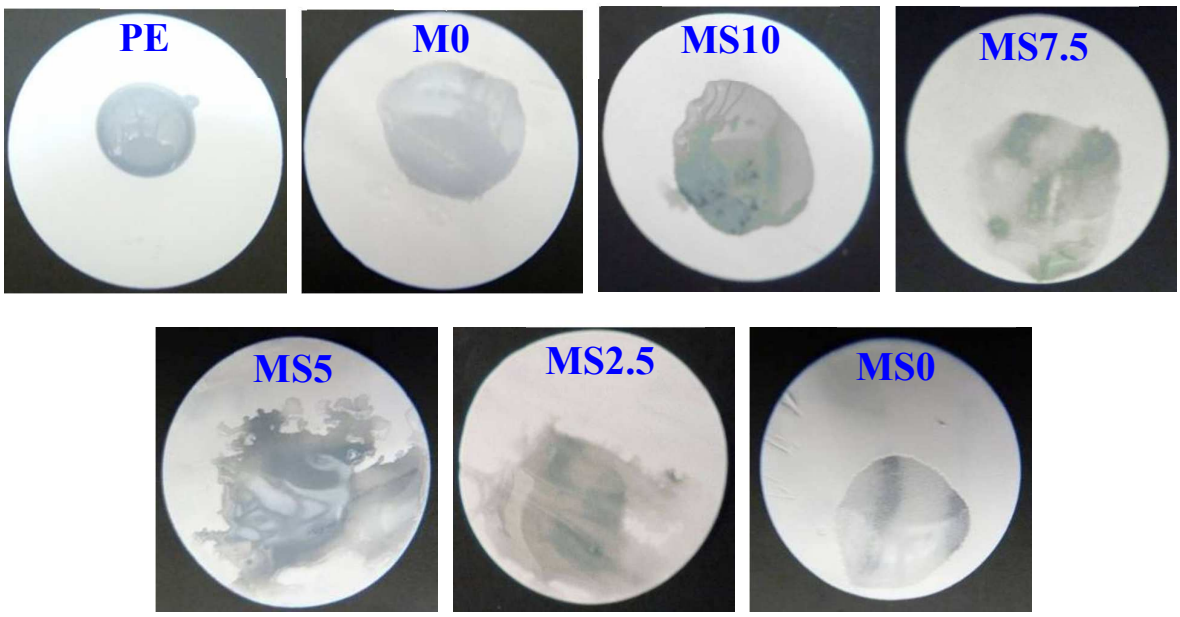

Fig. 4 Wettability of the PE separator and PE-supported P(MMA-AN-EA) membranes with different contents of nanoparticles.

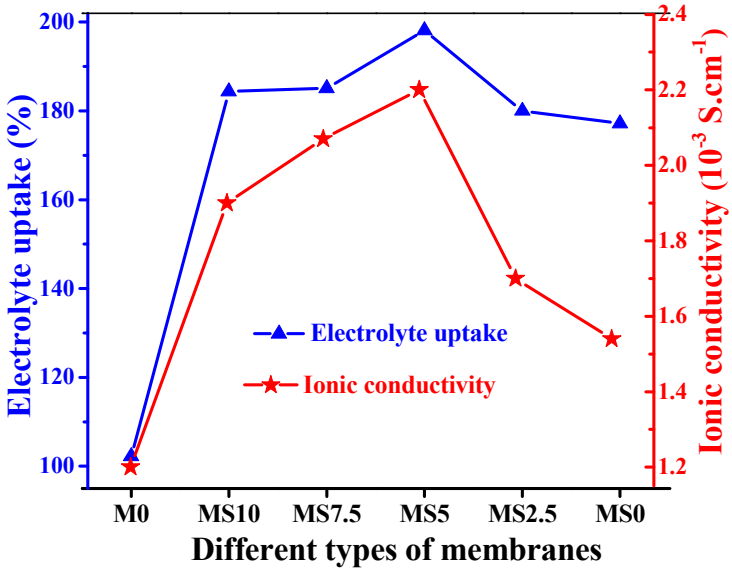

Fig. 5 Dependence of electrolyte uptake and ionic conductivity on the different types of membranes.

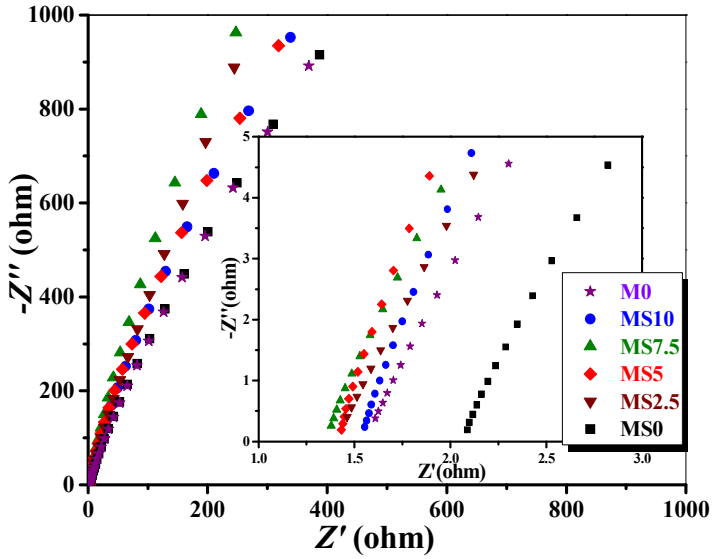

Fig. 6 Nyquist plots for the different GPEs in SS/GPE/SS cell at room temperature.

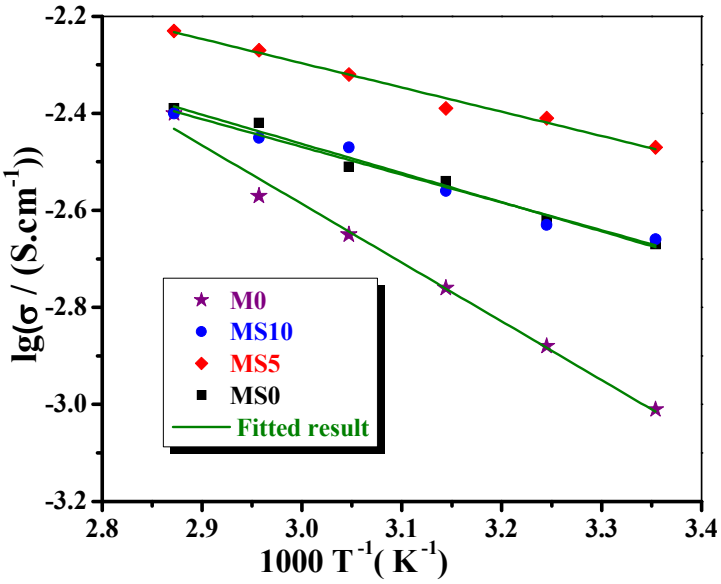

Fig. 7 Temperature dependence on the ionic conductivity of GPEs.

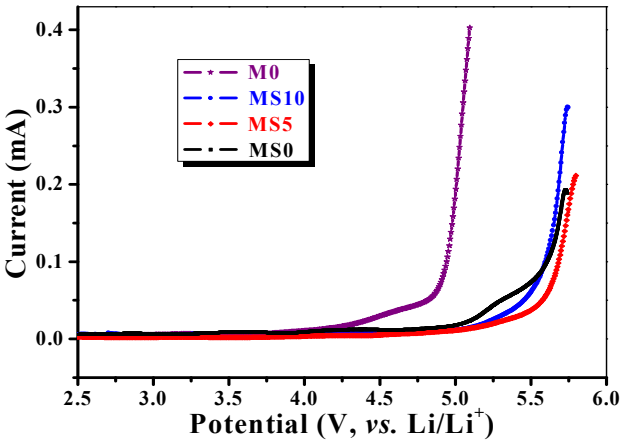

Fig. 8 Linear sweep voltammograms of various GPEs on stainless steel with the scanning rate of 1 $mV.s^{-1}$.

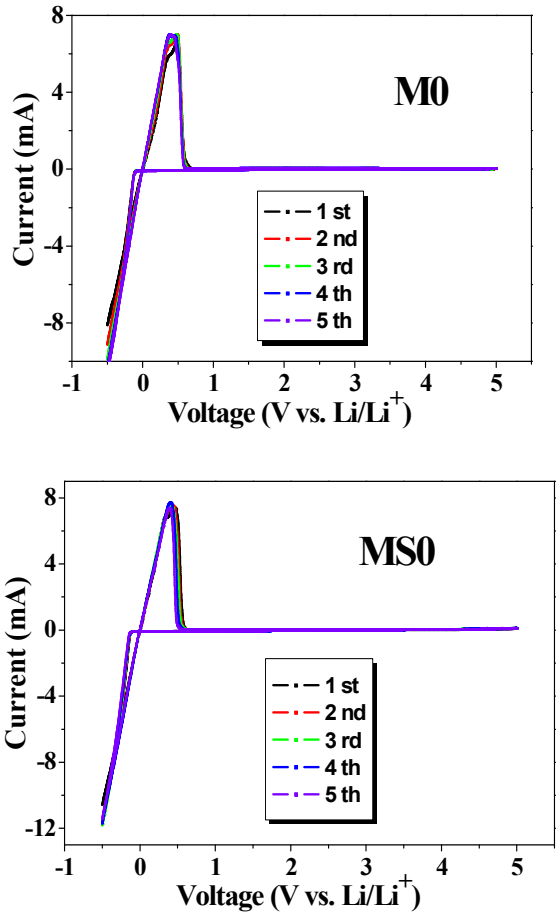

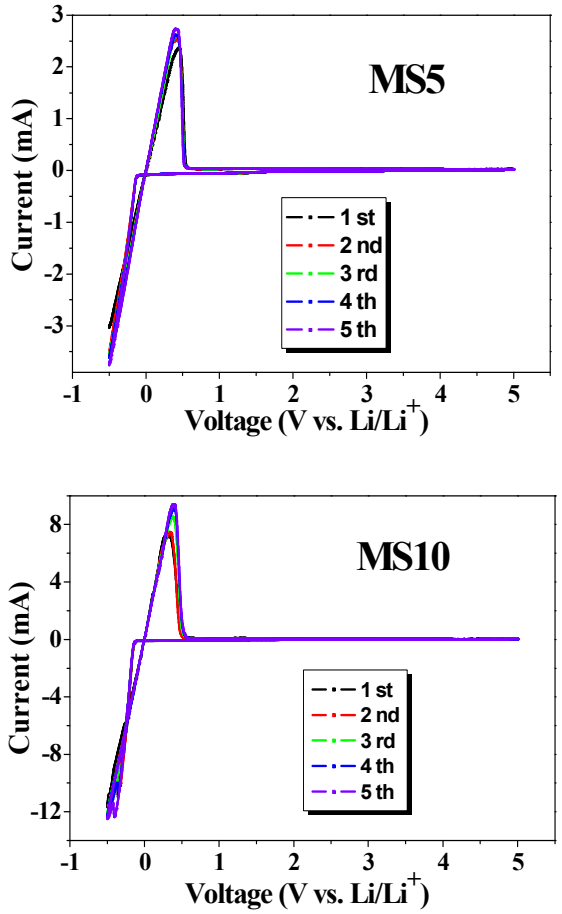

Fig. 9 Cyclic voltammograms of various GPEs for the cell Li/GPEs/SS in the voltage range of -0.5~5 V, scanning rate: 1 $mV.s^{-1}$.

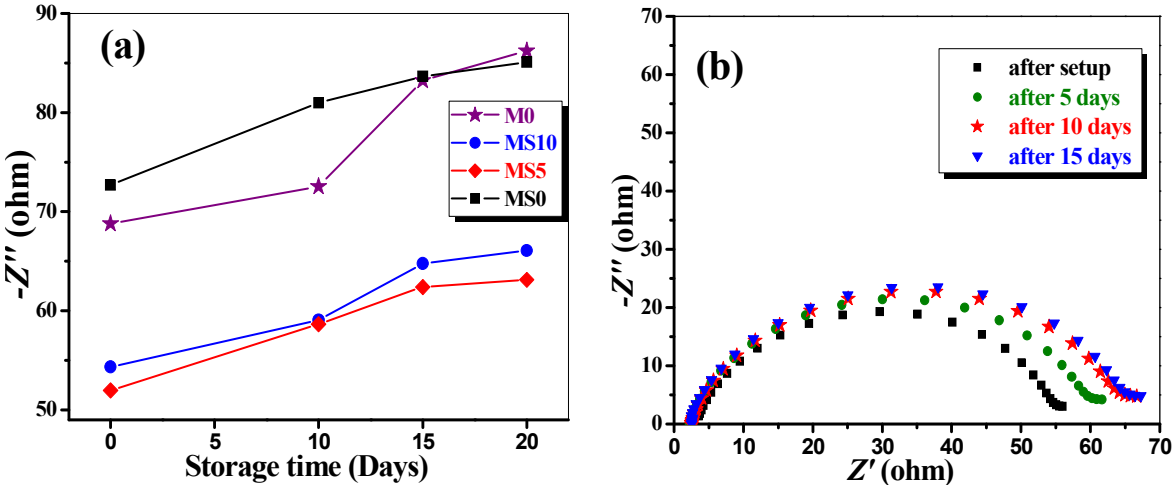

Fig. 10 (a) The dependence of interfacial resistance of Li/GPEs/Li on the storage time, and (b) the detail electrochemical impedance spectra for MS5 GPE.

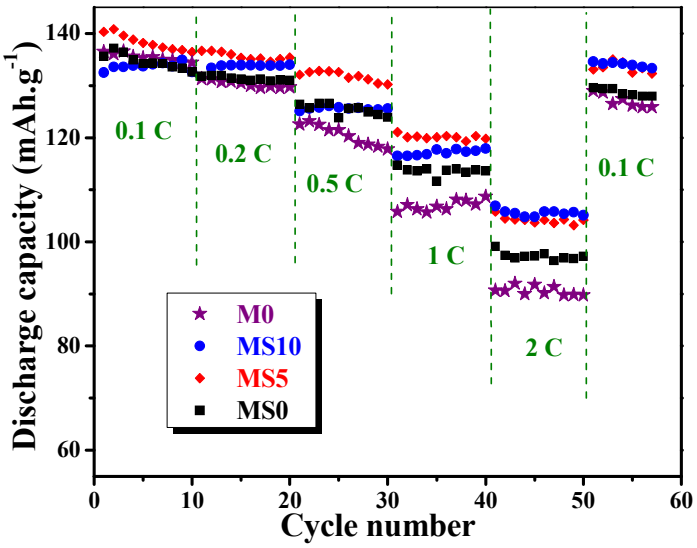

Fig. 11 Rate capability of $LiNi_{0.5}Mn_{1.5}O_4$ in various electrolytes at room temperature.

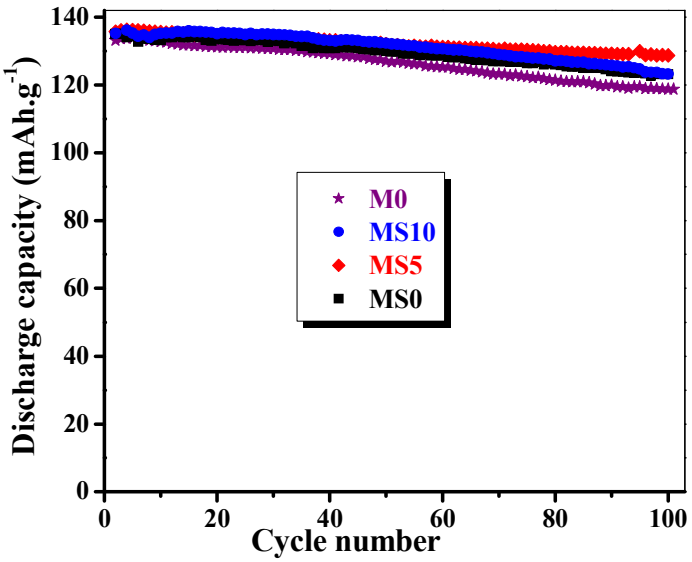

Fig. 12 Cyclic stability of $LiNi_{0.5}Mn_{1.5}O_4$ in various electrolytes under 0.2 C rate in the voltage range of 3.5 V and 5.0 V at room temperature.

Table Caption:

Table 1 The activation energy of different GPEs.

Table 1 The activation energy of different GPEs.

	M0	MS10	MS5	MS0
E_a (kJ.mol^{-1})	23.2	11.0	9.6	11.5